Surface waves at microwave frequencies excited on a zigzag metasurface

Helen J. Rance,* Thomas J. Constant, Alastair P. Hibbins, and J. Roy Sambles
Electromagnetic Materials Group, Department of Physics and Astronomy, University of Exeter, Exeter EX4 4QL, United Kingdom
(Received 4 April 2012; revised manuscript received 13 July 2012; published 28 September 2012)

Surface waves at microwave frequencies are excited on a zigzag metasurface formed from unit cells comprised of a pair of identical, alternately oriented, rhombic-shaped metal tubes. This particular symmetry leads to diffractive excitation, with polarization selectivity of different orders, of a family of surface waves. Furthermore, the expected band gap at the first Brillouin zone boundary is absent.

DOI: 10.1103/PhysRevB.86.125144 PACS number(s): 42.25.Bs, 42.25.Ja, 84.40.Az

I. INTRODUCTION

The symmetry of a metamaterial may be reduced through the modification of the shape and/or arrangements of the constituent subwavelength elements, allowing access to modes and phenomena unavailable in structures with higher symmetry. The excitation of "trapped-modes" (i.e., electromagnetic modes that are weakly coupled to free space) on planar metamaterials based on asymmetric split-rings resonators (ASRRs), for instance, has been reported at microwave,[1–4] near-ir,[5] terahertz,[6] and optical[7] frequencies, with uncharacteristically strong and narrow [high-quality (Q-) factor] resonances, being observed. In particular, when the incident electric field (E-field) is perpendicular to the plane of mirror symmetry of an array of ASRRs,[1] spectral selectivity, a special feature originating from asymmetrical structuring, has been reported. Further, the normal incidence reflection and transmission properties of circularly polarized radiation from and through chiral ASRRs[2] was shown to be highly dependent on the handedness and direction of incident radiation, attributable to the lack of mirror symmetry in this structure. Other phenomena arising from metamaterials with a high degree of asymmetry include metamaterial-induced transparency, which has been observed using individual two-gap ASRRs.[6] Here, the displacement of one gap from the central vertical axis reduces the symmetry, allowing for tuning of the amplitude and bandwidth of the transparency window. Further, a negative refractive index resulting from symmetry breaking of cut-wire pairs has been demonstrated at microwave frequencies,[8] and polarization-independent resonant absorption, arising from crossed trapezoid array structures,[9] has been observed at optical frequencies. In addition, the propagation of surface waves on periodic structures with reduced symmetries formed from arrays of slits[10] and holes[11] has shown that the reduced symmetry, which arises from the addition of a second periodicity or substructure within the unit cell, results in Fano-like phase resonances, not normally observed with their symmetric counterparts.

In the present study, the microwave response of a different reduced symmetry metasurface formed from an array of finite-height ($h = 20$ mm), geometrically identical rhombic-shaped elements (holes) is explored. The frequencies of the supported waveguide modes in the holes[12] provide the asymptotic limits for a family of supported transverse magnetic (TM) surface waves.[13] The surface waves on both surfaces couple through the structure and reradiate from the second surface giving the "enhanced transmission"[14] recorded in our experiments. The unit cell (solid line) comprises paired rhombic-shaped holes that are the mirror image of each other [Fig. 1(a)]. This provides a structure factor that reduces the symmetry of the system. Defining the plane of incidence to be the xz plane, this zigzag geometry is characterized by a surface modulation in the plane of the incident wave vector, with an orthogonal mirror plane, yz plane [dotted line, Fig. 1(a)].

The resulting zigzag metasurface structure allows for direct coupling of both p- and s-polarized incident radiation to surface modes. The necessary momentum enhancement is provided by the periodicity of the zigzag modulation in the plane of the surface, so no additional coupling-in mechanism is required as, for example, was necessary in previous "spoof" or "designer" surface wave experiments.[15] Another surprising phenomenon is also observed: polarization-selective excitation of individual surface wave bands, a direct consequence of the reduced symmetry of the system. In contrast to other studies such as the compound hole array work of Liu *et al.*,[11] in which the symmetry is reduced through the use of two different sized holes, the present structure is formed from geometrically identical holes, thus maintaining equivalent boundary conditions on every hole, with each hole having identical eigenmodes.

II. EXPERIMENTAL

The experimental sample (approximate size 360 × 360 mm) is manufactured using three-dimensional (3D) printing (ProJet™ HD 3000 rapid prototyping machine) and subsequent metallization. A collimated plane wave of microwave radiation is incident on the sample in the xz plane (i.e., containing the zigzag axis) using a horn antenna placed at the focus of a 2-m focal length spherical mirror [Figs. 1(b) and 1(c)]. The transmitted radiation is then collected by a similar spherical mirror and focused into a detector horn. At normal incidence ($\theta = 0^\circ$), the onset of diffraction from the zigzag pitch ($L = 16.5$ mm) occurs at 18.2 GHz, just below the cutoff of a single, infinite-length, rhombic-shaped waveguide, f_1 [Fig. 2(a)]. Diffraction from the orthogonal pitch ($S = 9.5$ mm) occurs at 31.6 GHz, which, since it is above the frequency of the second supported waveguide resonance, f_2 [Figs. 2(b) and 2(c)], is beyond the region of interest of this study. The microwave transmission spectra (grayscale) were recorded as a function of incident angle, θ (in incremental steps of $\theta = 0.2^\circ$); the resulting data provide information on the dispersion of the modes supported and are illustrated in Figs. 3(a) and 3(b) for TM (p-polarized) and transverse

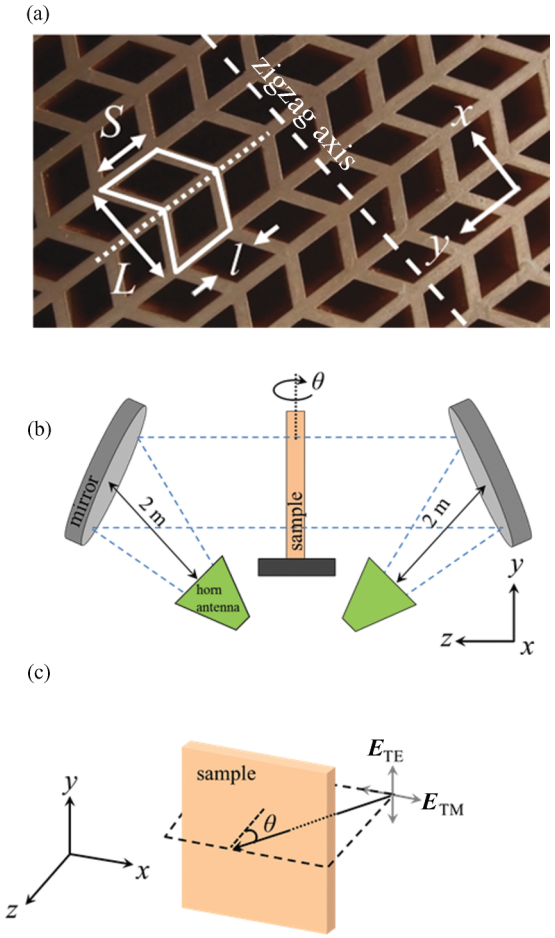

FIG. 1. (Color online) (a) Photograph of experimental sample with coordinate system. Plane of incidence (dashed line) and a plane of mirror symmetry (dotted line) are shown. The unit cell (solid line) is formed from paired rhombic-shaped holes, side length, $l = 7.0$ mm, zigzag pitch $L = 16.5$ mm and orthogonal pitch, $S = 9.5$ mm. (b) Schematic representation of experimental setup for transmission at normal incidence. (c) Schematic representation of plane of incidence and coordinate system used.

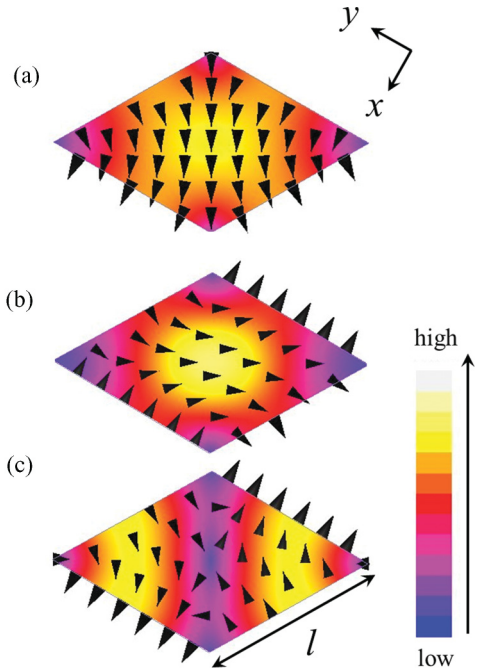

FIG. 2. (Color online) Predicted time-averaged (color map) and instantaneous (arrows) E-field profiles calculated over a surface parallel to the xy plane of the waveguide, plotted at a phase corresponding to maximum field enhancement, for the waveguide modes supported at (a) $f_1 = 18.33$ GHz and (b) $f_2 = 28.71$ GHz. Yellow regions (light gray) corresponds to high-field enhancement, and blue (medium gray) corresponds to a field magnitude of zero. To break the degeneracy and resolve the two modes supported at 28.71 GHz, a rhombic cross section with 60.001° corner has been modeled.

electric (TE; s-polarized) radiation with the plane of incidence containing the zigzag wave vector. Here, light and dark regions correspond to high and low transmissivity, respectively.

III. RESULTS AND DICUSSION

The frequencies of the waveguide resonances supported by each individual hole [the fundamental mode of which is a TE waveguide mode ($E_z = 0$) at $f_1 = 18.33$ GHz, Fig. 2(a), with two further degenerate TE modes supported at $f_2 = 28.71$ GHz Figs. 2(b) and 2(c)] are represented by horizontal dashed lines in Fig. 3. These hybridize with grazing diffracted orders (diagonal lines Fig. 3), and the resulting surface modes are highly dispersive, closely following the in-plane first and second diffracted light lines (solid and dashed diagonal lines, respectively) and asymptotically approach the limiting frequencies, dictated by f_1 and f_2, when they become strongly localized to the surface. Modeling of the eigenmodes[16] of the system reveals that, close to these limiting frequencies, the surface mode splits into symmetric (squares) and antisymmetric (crosses; Fig. 3) charge distribution, characteristic of coupled surface waves.[16] The predicted time-averaged E-field of these two modes is shown in the inset of Fig. 3(b), bottom left and bottom right, respectively. As is to be expected, further modeling of the transmissivity response shows that the separation of these two solutions is highly dependent on tube length. In this study the tube length is selected so that the two solutions converge on a single frequency, and the splitting of the symmetric and antisymmetric pair of coupled surface waves is not experimentally resolved.

One may effectively reduce the analysis of the band structure of this dual-pitch system to just two components of the zigzag grating profile: a very large amplitude, short-pitch component of period $L/2$ (i.e., closely spaced deep holes) convolved with a much weaker longer-pitch component of period L, associated with the different orientation of every other hole (a similar, detailed discussion of the band structure of deep gratings with compound structure can be found in Refs. 10, 17, and 18). Essentially the substructure holes of pitch $L/2$ give the necessary boundary conditions at the metal surface to support bound surface waves i.e., the inductive surface impedance[19] associated with the exponentially decaying fields at frequencies below the localized waveguide resonances within each hole. Then, the modulation of the grating in the plane of the incident wave vector associated with the zigzag geometry (pitch L) provides a mechanism for

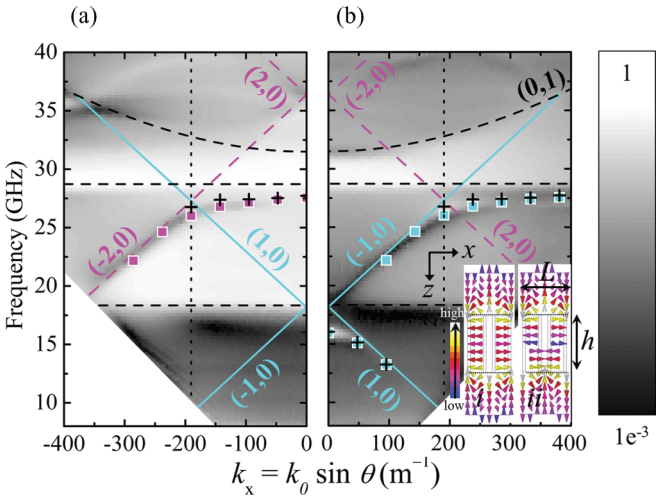

FIG. 3. (Color online) Experimental transmission data (grayscale) plotted on a log scale for (a) p- and (b) s-polarized incident radiation in a xz plane, recorded as a function of θ. Light and dark regions correspond to high and low transmissivity, respectively. The horizontal dashed lines represent the frequencies of the first (f_1) and second (f_2) supported TE waveguide modes. The solid and dashed diagonal lines represent the first- and second-order diffracted light lines, respectively. The dashed vertical lines indicate the Brillouin zone boundaries at $\pm\pi/L$ ($=k_g/2$). Inset: Predicted time-averaged E-field profiles plotted in the xz plane for (i) symmetric (predicted dispersion, squares) and (ii) antisymmetric (predicted dispersion, crosses) field solution. Yellow regions (light gray) correspond to high field enhancement, and blue (medium gray) corresponds to a field magnitude of zero.

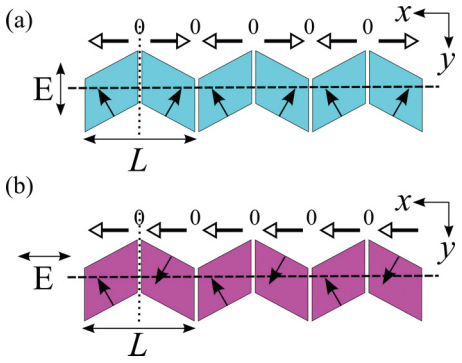

FIG. 4. (Color online) Schematic representation of the instantaneous E-field (solid arrows) for the surface mode supported at low frequencies for (a) s- and (b) p-polarized radiation incident in a plane containing the zigzag axis. Plane of incidence (dashed line) and mirror plane (dotted line) are shown. Open arrows represent the local component of the electric vector contained in the plane of incidence.

the incident radiation to diffractively couple to the surface modes. Scattering of the modes by the short-pitch component, $2k_g$ (where $k_g = 2\pi/L$), effectively increases the size of the Brillouin zone such that it is twice that associated with a system with a single periodicity, equal to L. Hence, the band structure may repeat within $\pm(\pi/(L/2))$, not $\pm\pi/L$. While the long-pitch component is too weak to cause any significant perturbation of the surface wave bands, it will introduce important band-folding effects. Hence, the originally nonradiative modes associated with the short-pitch component ($L/2$), become radiative through scattering introduced by the long-pitch component L, i.e., scattering by integer multiples of k_g. However, while this analysis is useful for describing the band structure of the eigenmodes of the system, it does not provide a full description for the origin of the polarization selectivity of the excitation of different surface wave bands, a property that can only be attributed to the unique symmetry of the zigzag geometry.

The orientation of the incident electric vector, with respect to the mirror plane of the geometry, is key to understanding the polarization-selective response of the array. First, consider when the electric vector lies perpendicular to the plane containing the incident wave vector (s-polarized radiation), i.e., the E-field of the incident radiation lies parallel to the plane of mirror symmetry. The schematic representation of the instantaneous E-field (solid arrows) in the low-frequency limit is shown in Fig. 4(a). Note that the local component of the electric vector contained **in the plane of incidence** (open arrows) switches direction at each mirror plane, a consequence of the alternation of the rhombic orientation of each hole. At low frequencies, the periodicity of the in-plane E-field component corresponds to a surface mode of wavelength, which is equal to the pitch of the structure, L. This surface wave, therefore, originates from in-plane scattering via $k_x = \pm k_g$. Its inherent periodicity associated with L dictates that it cannot be excited via scattering from $k_x = 0$. Therefore, this mode is seen to follow the $\pm(1,0)$ in-plane diffracted light lines [Fig. 3(b)], asymptotically approaching the frequency of the first supported waveguide mode f_1, then continuing to follow the diffracted light lines before asymptotically approaching the frequency of the second supported waveguide mode, f_2.

However, when the E-field vector is contained in the plane of incidence (p-polarized radiation), i.e., the E-field of the incident radiation is perpendicular to the mirror plane, the orientation of the E-field with respect to the mirror plane forbids the excitation of the mode schematically represented in Fig. 4(a). This is evident from the lack of p-polarized excitation of a mode associated with $\pm k_g$ scattering in Fig. 3(a). However, a surface wave, scattered from $k_x = \pm 2k_g$, is observed [Fig. 3(a)]. The schematic representation of the instantaneous E-field (solid arrows) associated with this mode, in the low-frequency limit, is shown in Fig. 4(b). Again, consider the component of the electric vector contained in the plane of incidence [open arrows, Fig. 4(b)]. For an excitation field with this polarization at low frequencies, the in-plane E-field component cannot switch direction in alternate holes. However, there still is a structure-induced periodicity in the local component of the electric vector contained in the plane of incidence (open arrows), with a periodicity *half* that of the long-pitch L. Hence, we observe a mode originate from the in-plane scattering via $k_x = 2k_g$. Due to the mirror symmetry of the structure, no polarization conversion may occur for the incident plane containing the zigzag grating vector; hence, the modes remain excited either via only p- or s-polarized radiation for all angles of incidence. Further, the polarization-selectivity of the excitation of different surface wave bands effectively introduces a Brillouin zone from $-k_g$ to k_g, twice that associated with the pitch of the structure L. It is, therefore,

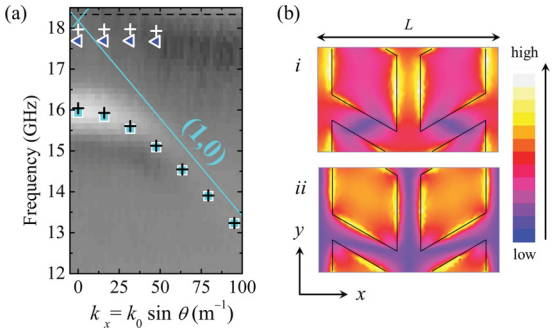

FIG. 5. (Color online) (a) Predicted dispersion of the modes near the band gap centered around $k_x = 0$. (b) Time-averaged E-field distribution of the symmetric solution of the (i) high-energy (triangles) and (ii) low-energy band (squares) at $k_x = 0$ plotted in the xy plane. Yellow (light gray) regions correspond to high field enhancement, and blue (medium gray) corresponds to a field magnitude of zero.

possible to make the general statement that s-polarized radiation may only couple to surface modes scattered from in-plane *odd* diffracted orders, while p-polarized radiation may only couple to surface modes scattered from in-plane *even* diffracted orders.

In addition to the expected band gap at the effective Brillouin zone boundaries $k_x = \pm k_g$ associated with the short-pitch component $(L/2)$, it is expected that band gaps will appear at points where two modes cross. However, the presence of the mirror plane forbids the existence of the band gap at $k_x = k_g/2$; the supported surface wave, associated with a $3k_g$ grating component, resulting from the coupling of two surface mode bands via scattering from $-k_g$ and $2k_g$, has a wavelength equal to $2/3L$. Owing to the symmetry of the zigzag geometry, the two possible standing wave solutions in the plane of the surface with this periodicity have the same energies. The two field solutions are, therefore, degenerate, and no band gap is observed. A band gap is, however, observed at $k_x = 0$. At this point surface modes couple together via scattering from $-k_g$ and $+k_g$ grating components leading to a standing wave of wavelength equal to the pitch of the grating L, associated with the $2k_g$ component. Here, two different standing wave solutions are possible; their predicted dispersion is shown in Fig. 5(a). Note that the different energy solutions are a result of a corrugation in the plane of the surface; the highest-energy band (triangles and white crosses) has high fields (yellow/light gray regions) centered on the metal regions in between the holes Fig. 5(b) i, while the lowest-energy band (squares and black crosses) can be found by displacing the nodes for the aforementioned solution by a quarter of the pitch, such that regions of high field (yellow/light gray regions) are centered over the holes [Fig. 5(b) ii].

IV. CONCLUSIONS

In conclusion, we have studied the intriguing behavior of bound TM surface waves propagating on a reduced symmetry metasurface with zigzag geometry. Characterized by a modulation in the plane of the incident wave vector and an orthogonal mirror plane, the zigzag metasurface is formed from unit cells comprised of a pair of identical, alternately oriented rhombic-shaped metal tubes. The correct boundary conditions to support the surface modes are provided by the inductive surface impedance associated with the exponentially decaying fields at frequencies below the localized waveguide resonances within each hole, while their paired arrangement creates the symmetry specific to the zigzag geometry. Diffractive excitation, with polarization selectivity of different orders, of a family of surface waves is observed. Furthermore, it is noted that the expected band gap at the first Brillouin zone boundary is absent.

ACKNOWLEDGMENT

The authors acknowledge the support of the EPSRC Grant No. EP/G022550/1.

*Corresponding author: h.j.rance@ex.ac.uk

[1] V. A. Fedotov, M. Rose, S. L. Prosvirnin, N. Papasimakis, and N. I. Zheludev, Phys. Rev. Lett. **99**, 147401 (2007).
[2] E. Plum, V. A. Fedotov, and N. I. Zheludev, Appl. Phys. Lett. **94**, 131901 (2009).
[3] R. Abdeddaim, A. Ourir, and J. de Rosny, Phys. Rev. B **83**, 033101 (2011).
[4] M. Kang, H.-X. Cui, Y. Li, B. Gu, J. Chen, and H.-T. Wang, J. Appl. Phys. **109**, 014901 (2011).
[5] K. Aydin, I. M. Pryce, and H. A. Atwater, Opt. Express **18**, 13407 (2010).
[6] R. Singh, I. A. I. Al-Naib, Y. Yang, D. R. Chowdhury, W. Cao, C. Rockstuhl, T. Ozaki, R. Morandotti, and W. Zhang, Appl. Phys. Lett. **99**, 201107 (2011).
[7] V. R. Tuz, S. L. Prosvirnin, and L. A. Kochetova, Phys. Rev. B **82**, 233402 (2010).
[8] S. N. Burokur, A. Sellier, B. Kanté, and A. de Lustrac, Appl. Phys. Lett. **94**, 201111 (2009).
[9] K. Aydin, V. E. Ferry, R. M. Briggs, and H. A. Atwater, Nat. Commun. **2**, 517 (2011).
[10] H. J. Rance, O. K. Hamilton, J. R. Sambles, and A. P. Hibbins, Appl. Phys. Lett. **95**, 041905 (2009).
[11] Z. Liu and G. Jin, J. Appl. Phys. **106**, 063122 (2009).
[12] P. L. Overfelt and C. S. Kenney, IEEE Trans. Microwave Theory Tech. **38**, 934 (1990).
[13] J. B. Pendry, L. Martín-Moreno, and F. J. Garcia-Vidal, Science **305**, 847 (2004).
[14] H. F. Ghaemi, T. Thio, D. E. Grupp, T. W. Ebbesen, and H. J. Lezec, Phys. Rev. B **58**, 6779 (1998).
[15] A. P. Hibbins, B. R. Evans, and J. R. Sambles, Science **308**, 670 (2005).
[16] HFSS, software version 13 (Ansys Corporation. Canonsburg, PA).
[17] A. P. Hibbins, J. R. Sambles, and C. R. Lawrence, Appl. Phys. Lett. **80**, 2410 (2002).
[18] A. P. Hibbins, I. R. Hooper, M. J. Lockyear, and J. R. Sambles, Phys. Rev. Lett. **96**, 257402 (2006).
[19] D. Sievenpiper, in *Metamaterials: Physics and Engineering Exploration*, edited by N. Engheta and R. W. Ziolkowski (Wiley-Interscience, Hoboken, NJ, 2006), Chap. 11, p. 289.